

PAPER • OPEN ACCESS

## Temperature dependence of electrical properties of electrodeposited Ni-based nanowires

To cite this article: R Dost *et al* 2017 *J. Phys.: Conf. Ser.* **902** 012010

View the [article online](#) for updates and enhancements.

### Related content

- [Tuning of operation mode of ZnO nanowire field effect transistors by solvent-driven surfacetreatment](#)  
Woojin Park, Woong-Ki Hong, Gunho Jo et al.
- [Nanolithography based contacting method for electrical measurements on single templatesynthesized nanowires](#)  
S Fusil, L Piraux, S Mátéfi-Tempfli et al.
- [Investigation on P-N dual acceptor doped p-type ZnO thin films and subsequent growth of pencil-like nanowires](#)  
R Amiruddin, Sebin Devasia, D K Mohammedali et al.

# Temperature dependence of electrical properties of electrodeposited Ni-based nanowires

**R Dost, D A Allwood and B J Inkson**

Dept. of Materials Science & Engineering, University of Sheffield, Sheffield, UK

E-mail: r.dost@sheffield.ac.uk

**Abstract.** The influence of annealing on the microstructure and the electrical properties of cylindrical nickel-based nanowires has been investigated. Nanowires of nickel of nominally 200 nm diameter and of permalloy (Py) of nominally 70 nm were fabricated by electrochemical deposition into nanoporous templates of polycarbonate and anodic alumina, respectively. Characterization was carried out on as-grown nanowires and nanowires heat treated at 650°C. Transmission electron microscopy and diffraction imaging of as-grown and annealed nanowires showed temperature-correlated grain growth of an initially nano-crystalline structure with  $\leq 8$  nm (Ni) and  $\leq 20$  nm (Py) grains towards coarser poly-crystallinity with grain sizes up to about 160 nm (Ni) and 70 nm (Py), latter being limited by the nanowire width. The electrical conductivity of individual as-grown and annealed Ni nanowires was measured in situ within a scanning electron microscope environment. At low current densities, the conductivity of annealed nanowires was estimated to have risen by a factor of about two over as-grown nanowires. We attribute this increase, at least in part, to the observed grain growth. The annealed nanowire was subsequently subjected to increasing current densities. Above 120 kA mm<sup>-2</sup> the nanowire resistance started to rise. At 450 kA mm<sup>-2</sup> the nanowire melted and current flow ceased.

## 1. Introduction

When Masuda *et al.* obtained controlled nanoporous alumina templates in 1995 [1] the fabrication of electrodeposited metallic nanowires was set to become commonplace. With time, nanowires with increasing complexity were grown, such as modulated shape [2] and composition [3, 4]. Using magnetic materials, they are still actively investigated today, mainly due to their various promising applications ranging from high-density magnetic recording [5] to high-frequency devices [6], passing by sensors [7] and biomedical applications [8]. However, the small size, fragility and particular features of cylindrical magnetic nanowires – such as high shape anisotropy, small magnetic volume, dipolar magnetic interactions between them when in array conformation, and electronic properties – present challenges to their characterization. The scientific community has been studying their structural [9], magnetic [3, 10] and electrical properties [4, 11] with great interest.

On another note, the emerging field of magnon spintronic devices promises to become a viable alternative to the stagnating complementary metal-oxide semiconductor (CMOS) based data processing technology [12, 13]. One way to help drive its miniaturization down to the nanoscale is a microwave-driven nanosized antenna that can excite high-wave-number and small-wavelength spin waves in ferromagnetic wave guides [14]. However, the choice of patterning technique in magnonic device fabrication has largely been electron-beam lithography. The more recent idea to complement magnonic structures with electrodeposited nanowires is founded on the constant strive to improve their



design and efficiency. For instance, cylindrical magnetic nanowires have the potential to act as a resonant transducer that couples a uniform external microwave field to propagating spin waves. Au *et al.* have shown that the resonantly driven magnetization precession of a cylindrical transducer creates a local dynamic dipolar field that can exceed that of the incident microwave field by one order of magnitude. Coupling strength and spin wave excitation are amplified [15].

In view of controlling the functional properties of nanosized cylindrical magnetic microwave-to-spin-wave transducers, here we study the effect of heat treatment on the grain size of nickel-based cylindrical nanowires and on their electrical properties. Effects on the magnetic properties were also studied and will be published elsewhere.

## 2. Sample preparation

A nanoporous anodic alumina (AAO) template with about 70 nm pore diameter and 20 nm pore spacing was prepared from a 100  $\mu\text{m}$  thick aluminum sheet (Goodfellow<sup>®</sup>, 99.99% pure). At first, the aluminum was polished in a 1:4 parts solution of perchloric acid and ethanol at 2–3 Adc for a few seconds, then anodized in an aqueous solution of 0.3 mol/l oxalic acid and 0.05 mol/l phosphoric acid at 33 V for 3 h. The two alumina layers were then separated with mercury(II) chloride and the barrier layer was removed in 0.5 mol/l phosphoric acid for 90 min. A VoltaLab<sup>®</sup> PGZ 402 voltammetry cell was used to perform the electrochemical deposition of Ni-based nanowires at a DC potential of -1.2 V for 45 min. Solutions for the nickel electrodeposition contained 90 g/l NiSO<sub>4</sub>, 30 g/l H<sub>3</sub>BO<sub>3</sub>, 5 g/l L-ascorbic acid and 1 wt% gelatin, and for the electrodeposition of Ni-Fe 80/20 wt% permalloy (Py) contained 90 g/l NiSO<sub>4</sub>, 13.5 g/l FeSO<sub>4</sub>, 30 g/l H<sub>3</sub>BO<sub>3</sub> and 5 g/l L-ascorbic acid.

Cylindrical Ni nanowires (200 nm nominal diameter) were electrochemically deposited in a single nanoporous polycarbonate template (Whatman<sup>®</sup> Nuclepore). Cylindrical Py nanowires (70 nm nominal diameter) were electrochemically deposited in the aforescribed AAO. Figure 1a shows the nanoporous structure of an AAO template, and figure 1b depicts electrodeposited Py nanowires, which grew bottom-up about halfway into the template pores. The nanowires obtained are typically 5–9  $\mu\text{m}$  long. Scanning electron microscopy (SEM) imaging was carried out on a FEI Nova<sup>™</sup> NanoSEM 450.

Electrodeposited templates were selectively subjected to a heat treatment in a furnace under a protective N<sub>2</sub> atmosphere. The temperature was raised to 650°C, held for one hour, then allowed to naturally cool. We refer to *as-grown* nanowires when not heat treated and *annealed* when heat treated.

Some Ni and Py nanowires were released by dissolving their templates in chloroform and 1M NaOH solution, respectively, then drop cast from suspension onto a substrate. The nanowires dispersed randomly and came to rest either isolated or in bundles (figure 1c), depending on the interplay of surface energies and cohesive forces between individual nanowires and the substrate.

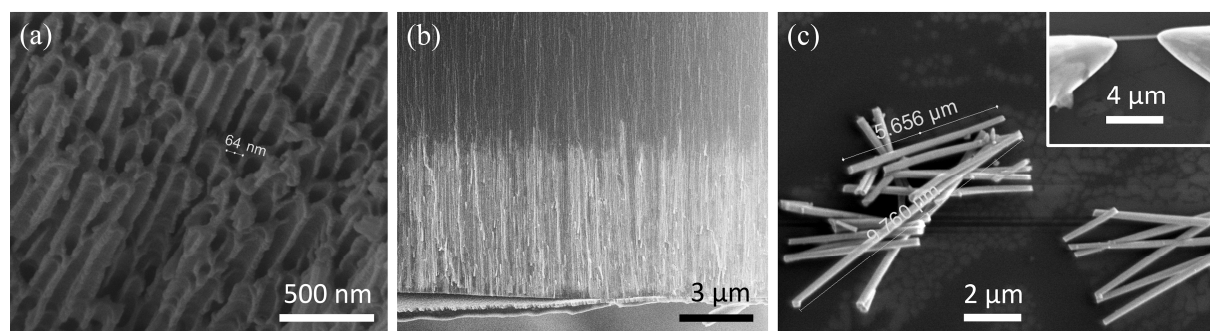


**Figure 1.** (a) SEM image of nanoporous AAO template. (b) He-ion SE image of electro-deposited AAO template. Permalloy nanowires grew bottom-up halfway inside the pores (bright contrast). (c) Randomly organized nickel nanowires after drop casting from chloroform suspension. Inset: Tungsten tips making electric contact with a Ni nanowire.

### 3. Experimental results

Transmission electron microscopy (TEM) and diffraction imaging (JEOL JEM 3010) was used to characterize the grain sizes of Ni-based nanowires prior to and after heat treatment. The as-grown nanowires are nano-crystalline. Grain sizes are about 20 nm or less for permalloy (figure 2a) and 8 nm or less for nickel (figure 3a). Heat treatment induces grain growth. After 650°C annealing, permalloy nanowires feature large grains that can fill the entire nanowire width ( $\varnothing 70$  nm), forming a ‘bamboo structure’ (figure 2b) [16]. The thicker poly-crystalline nickel nanowires ( $\varnothing 200$  nm) grow grains up to 160 nm (figure 3b). The width of the annealed nanowire remained unaffected to within  $\pm 2$  nm, or 1%.

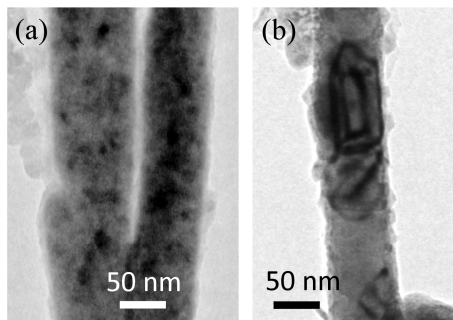


**Figure 2.** TEM images of  $\sim 80$  nm wide Py nanowires. (a) Two as-grown nanowires with grain sizes  $\leq 20$  nm. (b) After annealing at 650°C, the nanowire grew large grains up to its full width.

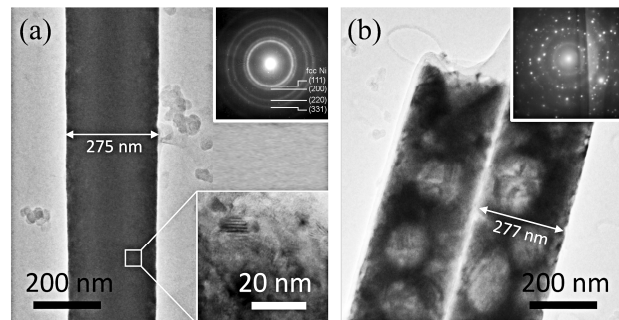


**Figure 3.** TEM images of  $\sim 275$  nm wide Ni nanowires. (a) Before annealing grain sizes are  $\leq 8$  nm (see magnified area). (b) After annealing at 650°C, grain sizes are up to  $\sim 160$  nm. Insets: Representative diffraction patterns.

The electrical conductivities of untreated and 650°C heat-treated individual Ni nanowires (275 nm diameter) were studied from current-voltage measurements. The nanowires were probed in a SEM environment by two Kleindiek MM3A-EM micromanipulators with tungsten probes (inset to figure 1c). All measurements used the same pair of probes with a tip-to-tip resistance ( $R_t$ ) of about 30  $\Omega$ . To make good mechanical contact with the nanowires, the tungsten tips applied a gentle vertical force. To make good electrical contact and minimize the effect of contact resistance, the actual IV measurements preceded one or more ‘burn-in’ bias sweeps where voltage was raised stepwise (up to  $\pm 5$  V) until total resistance ( $R$ ) reached a minimum. This process breaks down any oxide layer that may have been present on the nanowire surface [17] and yielded a repeatable total resistance to within  $\pm 2\%$  for the same kind of nanowires and same probe spacing ( $R_{nw} \cong \text{const}$ ). By implication, the uncertainty in  $R_c$  had to also be approximately equal to  $\pm 0.02 R$  – for any nanowire – albeit of unknown magnitude.

Figure 4a shows the IV curve of an as-grown nanowire at low forward-reverse biasing at 2.6  $\mu\text{m}$  probe spacing ( $L_1$ ) and figure 4b of an annealed nanowire at maximum forward biasing at 2.9  $\mu\text{m}$  probe spacing ( $L_2$ ). The as-grown nanowire exhibits a linear  $I(V)$  characteristic within the applied  $\pm 0.1$  V sweep, corresponding to current densities ( $J$ ) of 0–43  $\text{kA mm}^{-2}$ , with a total resistance  $R_1 = 38.7 \Omega$ . The 650°C annealed nanowire exhibited four distinct regimes during the high voltage sweep (see ①–④ in figure 4b).

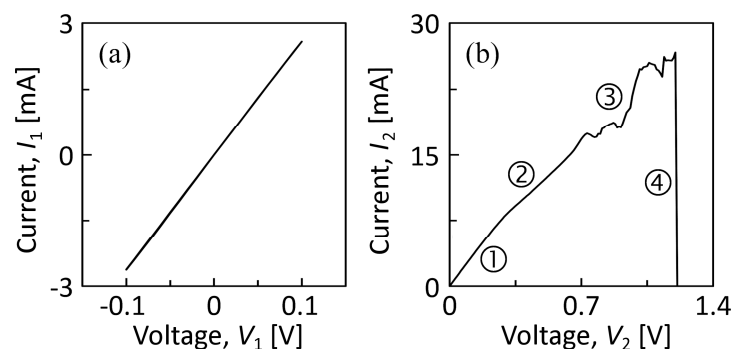


**Figure 4.** IV curves of (a) an individual as-grown Ni nanowire and (b) of an individual Ni nanowire annealed at 650°C.

At low biasing, corresponding to  $J = 0\text{--}120\text{ kA mm}^{-2}$ , total resistance  $R_2$  was  $34.9\ \Omega$  and ohmic in nature. This change corresponds to a 9.9% drop in total resistance for the annealed nanowire and cannot be fully ascribed to uncertainty in contact resistance alone, estimated at  $\pm 0.7\ \Omega$  for either measurement. At increased biasing, equal to  $J = 120\text{--}240\text{ kA mm}^{-2}$ ,  $R_2$  rose to  $51.7\ \Omega$ . Above  $240\text{ kA mm}^{-2}$ ,  $R_2$  fluctuated erratically until current flow abruptly ceased at  $450\text{ kA mm}^{-2}$ . As observed in situ during SEM imaging, the nanowire melted from excessive Joule heating.

The change in conductivity ( $\sigma$ ) between as-grown and annealed nanowires was estimated for an unknown but constant voltage drop ( $V_c$ ) across  $R_c$  by evaluating both IV curves in the low biasing regime at identical currents of  $2.58\text{ mA}$  (arbitrary). Given the same cross-sectional areas, the conductivity ratio of annealed ( $\sigma_{\text{nw2}}$ ) to as-grown nanowire ( $\sigma_{\text{nw1}}$ ) is  $\frac{\sigma_{\text{nw2}}}{\sigma_{\text{nw1}}} = \frac{L_2}{L_1} \left( \frac{R_1}{R_2} - \frac{R_c}{R_2} \right) \left( 1 - \frac{R_c}{R_2} \right)^{-1}$ . Assuming  $R_c \sim R_t$ , the 9.9% drop in total resistance corresponds to an increase in the annealed nanowire conductivity by +99%. Should  $R_c$  approach  $0.9 R_2$  then  $\sigma_{\text{nw2}}$  approached the Ni bulk conductivity of  $1.43 \times 10^7\text{ S m}^{-1}$  [18], corresponding to an increase in conductivity by +136%.

We conclude, the estimated increase in nanowire conductivity must be attributed, at least in part, to the observed grain growth with heat treatment. Larger grains mean fewer grain boundaries – sites of electron scattering, which contribute to electrical resistance. Magneto-optical Kerr effect magnetometry showed that the Ni and Py nanowires exhibit magnetic properties. The data will be detailed elsewhere.

#### 4. Conclusion

Here we show that the grain structure of magnetic cylindrical nanowires can be altered through heat treatment, which causes significant grain growth, tending towards a bamboo-microstructure. This in turn reduces grain boundary surface area with an approximately two-fold increase in electrical conductivity for the  $650^\circ\text{C}$  annealed nickel nanowires. Current densities above about  $120\text{ kA mm}^{-2}$  lead to Joule heating and degrade conductivity until structural failure.

#### Acknowledgement

This work was supported by the Engineering and Physical Sciences Research Council [grant number EP/L020696/1].

#### References

- [1] Masuda H and Fukuda K 1995 *Science* **268** pp 1466–8
- [2] Lee W, Ji R, Gösele U and Nielsch K 2006 *Nat. Mater.* **5** pp 741–7
- [3] Moura K O *et al.* 2016 *Sci. Rep.* **6** 28364
- [4] Elawayeb M, Peng Y, Briston K J and Inkson B J 2012 *J. Appl. Phys.* **111** 034306
- [5] Irshad M I, Ahmad F and Mohamed N M 2012 *AIP Conf. Proc.* (Malaysia, Melville: AIP) p 625
- [6] Frake J C, Kano S, Ciccarelli C, Griffiths J, Sakamoto M, Teranishi T, Majima Y, Smith C G and Buitelaar M R 2015 *Sci. Rep.* **5** pp 1–6
- [7] Chena X, Wonga C K Y, Yuan C A and Zhanga G 2013 *Sensor Actuat. B: Chem.* **177** pp 178–95
- [8] Patolsky F, Zheng G and Lieber C M 2006 *Nanomedicine* **1** pp 51–65
- [9] Maaz K *et al.* 2010 *Nanoscale Res. Lett.* **5** pp 1111–17
- [10] Encinas-Oropesa A, Demand M and Piraux L 2001 *Phys. Rev. B* **63** 104415
- [11] Wu J, Yin B, Wu F, Myung Y and Banerjee P 2014 *Appl. Phys. Lett.* **105** 183506
- [12] Kruglyak V V, Demokritov S O and Grundler D 2010 *J. Phys. D: Appl. Phys.* **43** 264001
- [13] Lenk B, Ulrichs H, Garbs F and Münzenberg M 2011 *Phys. Rep.* **507** pp 107–36
- [14] Ciubotaru F 2012 Thesis: *Spin-wave excitation by nano-sized antennas* (University of Kaiserslautern)
- [15] Au Y, Ahmad E, Dmytriiev O, Dvornik M, Davison T and Kruglyak V V 2012 *Appl. Phys. Lett.* **100** 182404
- [16] Hummelgård M *et al.* 2010 *Nanotechnology* **21** 165704
- [17] Krishnan S, Stefanakos E and Bhansali S 2007 *Thin Solid Films* **516** pp 2244–50
- [18] Laubitz M J, Matsumura T and Kelly P J 1976 *Can. J. Phys.* **54** pp 92–102